

Different reactions of Southern Ocean phytoplankton size classes to iron fertilization

Linn J. Hoffmann,¹ Ilka Peeken, and Karin Lochte

Leibniz Institute of Marine Science at the University of Kiel, Duesternbrooker Weg 20, 24105 Kiel, Germany

Philipp Assmy

Alfred Wegener Institute for Polar and Marine Research, Am Handelshafen 12, 27570 Bremerhaven, Germany

Marcel Veldhuis

Royal Netherlands Institute for Sea Research, P.O. Box 59, 1790 AB Den Burg, Texel, The Netherlands

Abstract

During the European Iron Fertilisation Experiment (EIFEX), performed in the Southern Ocean, we investigated the reactions of different phytoplankton size classes to iron fertilization, applying measurements of size fractionated pigments, particulate organic matter, microscopy, and flow cytometry. Chlorophyll *a* (Chl *a*) concentrations at 20-m depth increased more than fivefold following fertilization through day 26, while concentrations of particulate organic carbon (POC), nitrogen (PON), and phosphorus (POP) roughly doubled through day 29. Concentrations of Chl *a* and particulate organic matter decreased toward the end of the experiment, indicating the demise of the iron-induced phytoplankton bloom. Despite a decrease in total diatom biomass at the end of the experiment, biogenic particulate silicate (bPSi) concentrations increased steadily due to a relative increase of heavily silicified diatoms. Although diatoms $>20 \mu\text{m}$ were the main beneficiaries of iron fertilization, the growth of small diatoms (2–8 μm) was also enhanced, leading to a shift from a haptophyte- to a diatom-dominated community in this size fraction. The total biomass had lower than Redfield C : N, N : P, and C : P ratios but did not show significant trends after iron fertilization. This concealed various alterations in the elemental composition of the different size fractions. The microplankton ($>20 \mu\text{m}$) showed decreasing C : N and increasing N : P and C : P ratios, possibly caused by increased N uptake and the consumption of cellular P pools. The nanoplankton (2–20 μm) showed almost constant C : N and decreasing N : P and C : P ratios. Our results suggest that the latter is caused by a shift in composition of taxonomic groups.

The Southern Ocean is one of the three High Nutrient Low Chlorophyll (HNLC) regions of the world's oceans, where macronutrients abound but phytoplankton growth is limited by the availability of iron (Martin et al. 1990).

¹ Corresponding author (lhoffmann@ifm-geomar.de).

Acknowledgments

We thank Captain U. Pahl and the crew of RV *Polarstern* for their support. Without the help of V. Smetacek (chief scientist), H. Leach, V. Strass, H. Prandke, B. Cisewski (CTD sampling), and the other cruise participants, our work would have been impossible. Special thanks to K. Nachtigall, C. Krieger, S. Krug, and A. Kähler for their help with HPLC measurements. We also thank K. Nachtigall and P. Fritsche for POC/PON, POP, and bPSi measurements. The manuscript was greatly improved by the comments of two anonymous reviewers. This research was funded by the German Research Foundation (DFG) grant PE_565_5 awarded to Ilka Peeken.

In situ iron fertilization experiments have been performed in all HNLC regions and all of them have in common that they induced strong phytoplankton blooms (see review in de Baar et al. 2005). The massive increase in chlorophyll *a* (Chl *a*) concentrations was mainly due to large or chain-forming diatoms, which benefit most from iron fertilization. Because iron uptake is dependent on cell surface area, smaller cells are favored under low iron concentrations due to their higher surface-to-volume ratios (Hudson and Morel 1990; Sunda and Huntsman 1997). The natural phytoplankton community of the iron-depleted Southern Ocean is therefore dominated by pico- and nanophytoplankton (Gervais et al. 2002). The small diatom *Chaetoceros brevis* did not change its growth rates under different iron concentrations in laboratory experiments, leading to the assumption that this species is not iron limited under natural conditions (Timmermans et al. 2001).

Once iron becomes available, larger cells can increase their abundance due to increased growth rates (Timmermans et al. 2001, 2004) and better grazing protection. Mesozooplankton, which could feed effectively on these large diatoms, have relatively long generation times and therefore cannot control this fast-growing biomass. Microzooplankton, on the other hand, which have much shorter generation times, are too small to effectively consume large diatoms (Coale et al. 1996). There is evidence from the equatorial Pacific that growth rates of smaller phytoplankton groups were also stimulated, but could not build up high biomasses because of a concurrent increase in grazing pressure (Coale et al. 1996; Cavender-Bares et al. 1999). The overall effect of these changes leads to a shift in phytoplankton composition from an assemblage dominated by pico- and nanophytoplankton toward a nano- and microphytoplankton-dominated one (Gall et al. 2001a; Gervais et al. 2002).

Iron plays a major role in photosynthetic metabolism. Under low iron concentrations, the cellular chlorophyll concentrations and the efficiency of photosynthetic electron transfer (Fv/Fm) are known to be lower compared with high-iron conditions (Geider and LaRoche 1994). Besides enhanced growth rates, the natural phytoplankton community shows an increase in Fv/Fm (Boyd et al. 2000; Gervais et al. 2002; Coale et al. 2004) and higher cellular chlorophyll concentrations with iron fertilization in the Southern Ocean (Veldhuis and Timmermans unpubl. data). The increase in cellular chlorophyll concentrations is higher in larger cells, again indicating that these cells are more iron limited than smaller ones (Veldhuis and Timmermans unpubl. data).

Regions of the Southern Ocean where diatoms dominate the phytoplankton community have lower than Redfield C : P and N : P ratios, while those dominated by *Phaeocystis* exceed the Redfield ratio (Arrigo et al. 1999, 2002). Laboratory experiments have shown that the elemental composition of phytoplankton can differ significantly from the Redfield ratio and that diatoms in general have lower C : P and N : P ratios than other taxonomical phytoplankton groups (Ho et al. 2004; Klausmeier et al. 2004). The change in the elemental composition of the whole phytoplankton community may therefore be due to changing species composition. It is also known that the elemental composition of phytoplankton is variable, depending on the availability of macronutrients (Geider and La Roche 2002) and trace metals, such as iron (de Baar et al. 1997; Timmermans et al. 2004; Twining et al. 2004).

Changes in the elemental composition of phytoplankton during in situ iron fertilization experiments are of particular interest because the aim of these experiments is to increase biological production and carbon export. Carbon uptake and export is estimated by using the Redfield ratio so that even small deviations from this ratio will have significant effects on these calculations. Recent biogeochemical models differentiate between phytoplankton groups such as diatoms, pico/nanophytoplankton, and coccolithophores (Pasquer et al. 2005), and they require reliable information about possible changes in the group

composition and associated variations in the elemental ratios due to iron fertilization.

It is still unknown whether the observed changes in community structure and elemental composition would be sustained during long-term fertilization and would have lasting effects on the ecosystem structure. Most field research is concentrated on the microphytoplankton because of its dominant increase in biomass after iron fertilization, while the response of smaller phytoplankton size classes is not well understood. The aim of this study was to identify the growth response of all phytoplankton size classes, as well as changes in the elemental ratios and species composition during the iron fertilization experiment EIFEX in the Southern Ocean.

Material and methods

The European Iron Fertilisation Experiment (EIFEX) was an in situ iron fertilization experiment carried out during the Southern Hemisphere autumn (21 Jan 04–25 Mar 04). To perform the experiment in a relatively stable water mass, an eddy, localized around 50°S and 2°E, was chosen. The eddy center was fertilized twice with an acidified iron sulfate solution. The first fertilization was carried out on day one after the initial sampling to determine the prefertilization conditions. All stations were located inside the eddy. Stations within the fertilized patch will be called in-stations, while the so-called out-stations were located inside the eddy but outside the iron-fertilized waters. Iron concentrations were approximately 0.08–0.2 nmol L⁻¹ in the mixed layer before fertilization and reached about 2 nmol L⁻¹ after the first fertilization. At day 15, the same water mass, as identified by high Fv/Fm, was fertilized again because iron concentrations had now decreased to only 2–3 times background. After the second infusion, iron concentrations remained significantly higher throughout the experimental patch compared with prefertilization conditions (Croot pers. comm.).

The indicator for photosynthetic efficiency Fv/Fm is known to increase with iron fertilization. To distinguish fertilized from unfertilized waters, the photosynthetic efficiency of phytoplankton was measured by Fast-Repetition-Rate-Fluorescence (FastTracka; Röttgers et al. 2005). Additionally, higher in vivo fluorescence of Chl *a* compared with the surrounding waters was measured by a fluorescence laser system (LIDAR) from a helicopter (Cembella et al. 2005).

Samples for size fractionated POC, PON, POP, bPSi, and measurements for algae pigment analysis by high-performance liquid chromatography (HPLC) were taken at in-stations and out-stations from 20-m depth using a CTD rosette sampler. All determinations are single measurements. Fractionated filtration was carried out to determine particulate organic matter (POM; which includes POC, PON, and POP) and pigment concentrations in different size classes. For POC and PON measurements, precombusted GF/F (Whatman) filters were used; bPSi determination was done on cellulose acetate (CA) filters (Millipore). For determination of the total amount, samples were directly filtered on the GF/F filters (25 mm in diameter) or

Table 1. Solvent gradient used for HPLC measurements. Solvent A: 30% 1 mol L⁻¹ ammonium acetate, 70% methanol. Solvent B: 100% methanol.

Time (min)	Solvent A in %	Solvent B in %
0	65	35
1	50	50
12	15	85
15	0	100
20	0	100
25	65	35

CA filters of 0.8- μm pore size (25 mm in diameter) for BPSi, respectively. For size fractionation, samples were prefiltered through polycarbonate (PC) filters of the pore sizes 0.8 μm -, 2 μm -, 8 μm -, or a 20- μm gauze, each 47 mm in diameter. The larger surface area was chosen to avoid clogging of filters/gauze to prevent smaller cells from being retained. After filtration, the filters/gauze were rinsed and the filtrate was then filtered through GF/F or CA filters (each 25 mm in diameter) to collect the <0.8 μm , <2 μm , <8 μm , and <20 μm size fractions. The material on the 20- μm gauze was rinsed and collected on GF/F or CA filters for the >20- μm fraction. The fractions total, >20 μm , <20 μm , <8 μm , <2 μm , and <0.8 μm , were measured directly, the fractions 0.8–2 μm , 2–8 μm , 2–20 μm , and 8–20 μm were calculated by subtraction.

The volume of water filtered was between 1 and 6 L, depending on the amount of biomass in the water. POM filters were put in open Eppendorf tubes and immediately dried for at least 48 h in a drying oven. Afterward, the Eppendorf tubes were closed and stored with desiccant in closed plastic boxes. Immediately after filtration, the HPLC filters were stored in 1.5-mL cryo vials at -80°C until analysis.

POC/PON filters were exposed over night to 32% HCl to remove the inorganic carbon. The carbon and nitrogen content of the particulate, organic material was analyzed using a C/N Analyser (Euro EA Elemental Analyser) after Ehrhard and Koeve (1999). The POP content was determined colorimetrically using the method from Hansen and Koroleff (1999). BPSi was transformed to dissolved silicate by heating the filters in 0.1 mol L⁻¹ NaOH solution to 85°C for 2 h. The dissolved silicate was then determined colorimetrically (Hansen and Koroleff 1999).

The HPLC samples were measured using a Waters 600 controller combined with a photodiode array detector (PDA; Waters 996) and an auto sampler (Waters 717plus). The method used was modified after Barlow et al. (1997) (Table 1). As an internal standard, 100 μL canthaxanthin were added to each sample. Identification and quantification of the different pigments were carried out using the program EMPOWER by Waters.

The whole phytoplankton community composition was classified into taxonomical groups applying the CHEMTAX program (Mackey et al. 1996). All Chl *a* concentrations of specific phytoplankton groups reported in this article are estimates based on the concentrations of their

marker pigments according to this program. The input matrix was taken from Wright et al. (1996). This input matrix has been shown to provide reliable results, which correspond very well to cell counts in a former in situ iron fertilization experiment in the Southern Ocean (Peeken et al. unpubl. data). Nevertheless, we did not feel comfortable using these ratios for fractionated samples because it is likely that extremely different input ratios need to be considered for the various fractions. Therefore, fractionated samples are only presented as relative and absolute amounts of marker pigments.

At each station, 4-mL water samples for flow cytometric analysis of the phytoplankton composition were preserved with a drop of hexamine-buffered formaline solution on board and stored at -80°C until measurement. We tested this method in the past and found that the loss of cells for most groups was minor, ranging between 5% and 10%. This error is in the same range as for frozen samples reported by Vaultot et al. (1989). Flow cytometer samples were analyzed with a bench-top flow cytometer (Beckman Coulter XL-MCL) as described by Veldhuis and coworkers (Veldhuis and Kraay 2000). Samples were thawed immediately before analysis and up to 1.5-mL sample volume had to be analyzed because of the low phytoplankton density. Cell size, biovolume, and cell carbon were determined using size fractionated samples (Veldhuis and Timmermans unpubl. data). Chl *a* concentration per cell was determined from chlorophyll fluorescence derived by flow cytometry calibrated against direct chlorophyll measurements by HPLC. The carbon content of different groups was estimated using cell size. In order to avoid confusion of the carbon content of the autotrophic biomass with the directly measured carbon content of the entire plankton community, we will use a different notation. The carbon to Chl *a* ratio estimated by flow cytometry will be called C : Chl, while POC : Chl will be used for the ratio of directly measured particulate organic carbon to Chl *a* concentrations determined by HPLC.

For quantitative assessment of the phytoplankton assemblage, 200-mL water samples were preserved with hexamine-buffered formaline solution at a final concentration of 2% and stored at 4°C in the dark for microscopic analysis in the home laboratory. Due to the use of buffered formaline solution, the pH of the preserved samples was kept at in situ levels (pH 8). Cell counts were performed using inverted light and epifluorescence microscopy (Axiovert 25, Axiovert 135, and IM 35; Zeiss) according to the method of Utermöhl (1958). For phytoplankton cells >10 μm , water samples were settled in 50-mL sedimentation chambers (Hydrobios) for 48 h. For specifically counting diatoms <10 μm , solitary *Phaeocystis antarctica*, and *Emiliania huxleyi*, phytoplankton samples were settled in 10-mL sedimentation chambers for 72 h to assure that all cells had settled. Organisms were counted at magnifications of $\times 200$ –640 according to the size of the organisms examined. Each sample was examined until at least 500 cells had been counted. In order to acquire information on species-specific mortality, recognizable empty and broken diatom frustules were counted. Broken and empty diatom frustules were identified to species or genus level and

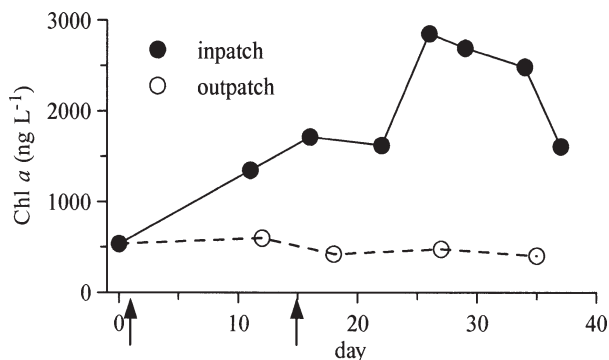


Fig. 1. Total Chl *a* concentration inside and outside the fertilized patch at 20-m depth. Arrows indicate days of iron fertilization.

otherwise grouped into size classes. Only broken diatom frustules of which >50% of the frustule was intact were counted. We cannot totally exclude dissolution of intact, empty, and broken frustules prior to examination of the samples by the storage, but the presence of empty and broken frustules of very delicate species, such as *Cylindrotheca closterium*, *Leptocylindrus mediteraneus*, and small *Chaetoceros* species, indicated that dissolution was of minor importance. Furthermore, some samples were counted again 9 months later and showed no significant differences in full, empty, as well as broken diatom cells between the two counts.

To investigate changes in the diatom community composition and its impact on bPSi accumulation, we compared heavily silicified species to the total diatom assemblage. The diatom species *Thalassiothrix antarctica*, *Fragilariopsis kerguelensis*, *F. obliquecostata* *ritzschieri*, *Thalassiosira lentiginosa*, *Thalassionema nitzschioides*, and *Thalassiosira gracilis* are known to occur in Antarctic sediments (Zielinski and Gersonde 1997). The accumulation of frustules of these species in the sediment is taken as

an indication of their strong silification, as compared with the majority of species that dissolve before reaching the sea floor. In the following, these species will be grouped as heavily silicified diatoms.

Results

Total plankton community response to iron fertilization—The total Chl *a* and POM concentrations showed a strong increase inside the fertilized patch, indicating a general biomass increase. The values were constantly higher than at the out-stations (Figs. 1 and 2). Chl *a* concentration increased more than fivefold through day 26, from 536 to 2853 ng L⁻¹, inside the patch and decreased thereafter. POC, PON, and POP concentrations roughly doubled during the first 30 days at the in-stations, while the concentrations at the out-stations did not increase and were constantly lower. Noticeable is a distinct dip at day 22 and a decline after day 30 inside the iron-fertilized patch; only bPSi showed a steady increase throughout the sampling period, reaching more than three times the initial concentrations (Fig. 2). At the out-stations, the bPSi concentrations were constantly lower but more variable compared with the POC, PON, and POP values. The POC : Chl *a* ratio of the total biomass decreased strongly inside the patch, from 180.8 to 55.5, at day 26 and increased thereafter to 86.9 (Fig 3).

While the Chl *a* concentrations at the out-stations gave the impression of a homogenous water mass surrounding the fertilized patch with approximately prefertilization conditions (Fig. 1), other data, like the bPSi concentrations (Fig. 2), the POC : Chl *a* ratio (Fig. 3), and pigments (Fig. 4B), showed larger variability. This might be partly explained by the occurrence of slightly different water masses, which lead to changes in temperature and salinity (Walter et al. 2005). Compared with the large changes following fertilization, the variability at the out-stations is relatively small. However, especially for the calculation of

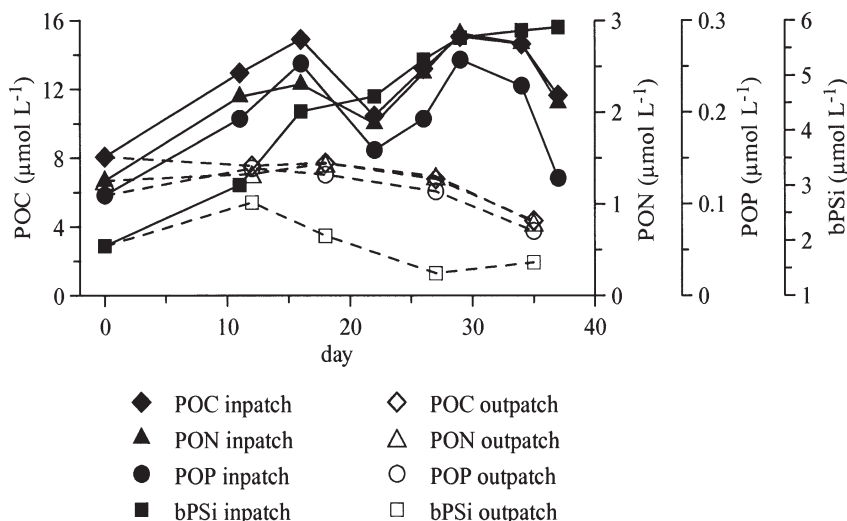


Fig. 2. Particulate organic carbon (POC), nitrogen (PON), phosphorus (POP), and biogenic silicate (bPSi) inside and outside the fertilized patch at 20-m depth.

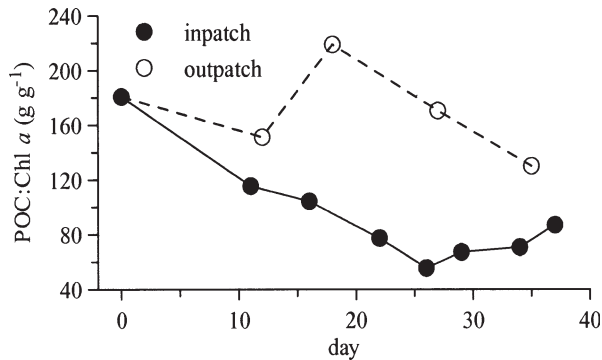


Fig. 3. Ratio of particulate organic carbon to Chl *a* inside and outside the fertilized patch at 20-m depth.

relative values and ratios, such as the percentage of total carbon and the elemental ratios, these minor deviations resulted in huge differences. We therefore omitted two stations that were clearly outliers and present the elemental ratios of three remaining out-stations as means and standard deviation in Fig. 6.

The CHEMTAX program (Mackey et al. 1996) provides estimates of the contribution of taxonomic phytoplankton groups to the total Chl *a* concentration based on their specific pigment composition. Using this method, we were able to distinguish between the seven phytoplankton groups chlorophytes, cyanobacteria, diatoms, dinoflagellates, pelagophytes, and two haptophyte types (*Phaeocystis* and *Emiliania huxleyi* type). According to these estimates, diatoms tended to dominate the phytoplankton community before and during the experiment and showed the greatest response to iron fertilization (Fig. 4A). They doubled their contribution to total Chl *a* from day 1 to day 26 (data not shown). The absolute diatom Chl *a* concentration increased five times in that time, while total diatom cell numbers increased almost three times (Fig. 4A). Based on the CHEMTAX results, the haptophyte type *Phaeocystis* was the second most abundant alga and increased its absolute Chl *a* concentration more than three times until day 29. Its relative abundance was about 20% of total Chl *a* and increased only marginally. Chlorophytes, cyanobacteria, dinoflagellates, and pelagophytes decreased in relative abundance because of the massive increase of diatom Chl *a* but did not change much in absolute Chl *a* concentrations and remained lower than 130 ng Chl *a* L⁻¹ during the experiment (Fig. 4A). The haptophyte type *Emiliania huxleyi* was the only group that decreased almost four times in absolute Chl *a* concentration during this experiment. Outside the fertilized patch, the phytoplankton community was also dominated by diatoms and absolute Chl *a* values of all phytoplankton groups remained more or less at the prefertilization level (Fig. 4B).

The number of full, broken, and empty total diatom cells increased up to days 29 and 32, respectively, and decreased thereafter (Table 2). Heavily silicified diatoms increased more than other diatoms during the experiment. This leads to an increase in the ratio of full heavily silicified diatoms to full total diatoms from 0.13 to 0.25 during the experiment. Empty and broken diatom frustules were counted as well

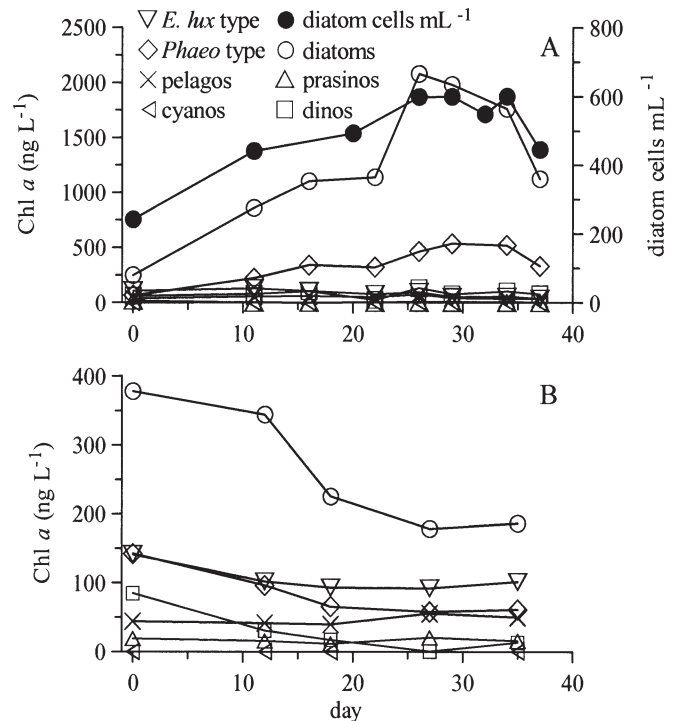


Fig. 4. Estimated Chl *a* concentration of the different phytoplankton groups based on the CHEMTAX program and total diatom cell numbers at 20-m depth (A) inside the fertilized patch and (B) outside the fertilized patch. Abbreviations are as follows: *E. hux* type for haptophyte type *Emiliania huxleyi*, *Phaeo* type for haptophyte type *Phaeocystis antarctica*, pelagos for pelagophytes, cyanos for cyanobacteria, prasinos for prasino-phytes, and dinos for dinophytes.

because they contribute to bPSi concentrations. The sum of full, empty, and broken heavily silicified diatoms to the sum of full, empty, and broken total diatoms increased from 0.24 to 0.46 in the fertilized patch.

The biomass distribution of the total diatom community showed a relative decrease in large *Chaetoceros* species, while *Thalassiothrix antarctica*, *Corethron inerme*, and *Rhizosolenoids* (including *Guinardia*, *Proboscia*, and *Rhizosolenia* species) increased their relative contribution. Other species, like *Fragilariopsis kerguelensis*, *Pseudo-nitzschia* spp., and *Dactyliosolen antarcticus*, were important in terms of biomass throughout the whole experiment, with only minor changes in their relative contribution to the total diatom biomass (Assmy et al. unpublished).

Analysis by flow cytometry—In general, four populations of phytoplankton differing in size and chlorophyll fluorescence were distinguished. The smallest cells had an equivalent spherical diameter (esd) of ca. 0.6 μm; furthermore, three groups of picophytoplankton with an esd of ca. 1.1 μm (pico-Euk), 1.2 μm (Euk I), and 1.8 μm (Euk II) and one group of the nanophytoplankton with an esd of 3.9 μm (Euk III) were present. No significant numbers of phycoerythrin-containing cyanobacteria were detected. Because of their extremely low numerical abundance, the smallest phytoplankton group detected (esd 0.6 μm and

Table 2. The ratio of bPSi : POC of the total community, full, empty, and broken total diatom cells mL⁻¹, and the ratio of heavily silicified diatoms to total diatoms from 20-m depth inside the fertilized patch.

Day	bPSi : POC	Total diatom cells (mL ⁻¹)			Heavily silicified cells : total cells			Sum of full, empty, and broken
		Full	Empty	Broken	Full	Empty	Broken	
0	0.24	242	61	13	0.13	0.22	0.28	0.24
11/16*	0.23/0.29*	441	49	13	0.11	0.26	0.42	0.28
20/22*	0.44*	492	86	29	0.17	0.28	0.28	0.30
26	0.40	598	87	31	0.19	0.31	0.36	0.33
29	0.38	599	95	34	0.16	0.23	0.33	0.26
32	-	548	123	28	0.22	0.33	0.30	0.40
34	0.40	599	90	26	0.16	0.41	0.45	0.39
37	0.50	445	60	27	0.25	0.45	0.34	0.46

* At days 16 and 22, only data for bPSi and POC are available.

contribution to total biomass of <1%) was not included in the data analysis. With respect to the chlorophyll content of the different phytoplankton groups, temporary higher cellular chlorophyll values (up to day 24) were observed in pico-Euk, Euk I, and in the largest group detected by flow cytometry (Euk III; Fig. 5). As a result of the minor changes in the cellular Chl *a* content, changes in the C : Chl ratio in these groups also can be observed. Whereas the C : Chl ratio of the picoeukaryotes (pico-Euk) remained virtually constant, Euk I showed higher C : Chl ratios in the second half of the experiment. Euk II responded with an increase in the ratio of C : Chl after day 26. Finally, the largest group (Euk III) showed a temporary decline in the C : Chl ratio during the first 24 days, rising to the initial

ratio thereafter. Noticeable is an abrupt change in cellular Chl *a* concentrations and the C : Chl ratio between days 24 and 26 especially in Euk I–III. At that time, distinct changes in many variables can be observed and may be explained by the beginning decay of the iron-induced bloom (Figs. 1, 3, 7, 8).

Changes in the elemental composition—As described above, the elemental ratios at the out-stations differed extremely. They are here presented as mean and standard deviations (Fig. 6). In response to iron fertilization, the elemental composition of the pico-, nano-, and microplankton, estimated from size-fractionated POC, PON, and POP measurements, followed different trends (Fig. 6). The C : N ratio of the total community as well as of the pico- and nanoplankton (<2 and 2–20 μm) showed only minor changes during the experiment. The values did not differ much from those of the out-stations, which were slightly lower than the Redfield C : N ratio (5.9 and 5.7). In contrast, the >20 μm size fraction had higher than Redfield values prior to fertilization (11.2), which decreased rapidly during the first 22 days and were constant thereafter at about 5.2.

The N : P ratio of the picoplankton increased during the experiment from close to Redfield ratios (16.1) to higher values (24.9) at the end. The N : P ratio of the nanoplankton was lower at the out-stations (about 6) than at the in-stations. It decreased from close to Redfield start values (17.1) at the in-stations to 7.7 on day 34 and was higher again at the last station (14.7). Microplankton N : P ratios showed a different trend. They increased from well below Redfield (4.9) to close to Redfield ratios after iron fertilization (14.6). At the out-stations, the ratios were constantly low at about 5. The N : P ratio of the total community in- and outside the fertilized patch was slightly lower than the Redfield ratio and did not reflect the changes in the different size classes.

The C : P ratio of the picoplankton did not show any trend and was constantly below the Redfield ratio, except for one outlier at the last station. The out-stations had a mean C : P ratio of 83, which is far below the Redfield ratio of 106. The C : P ratios of the nano- and microplankton and of the total community showed in general the

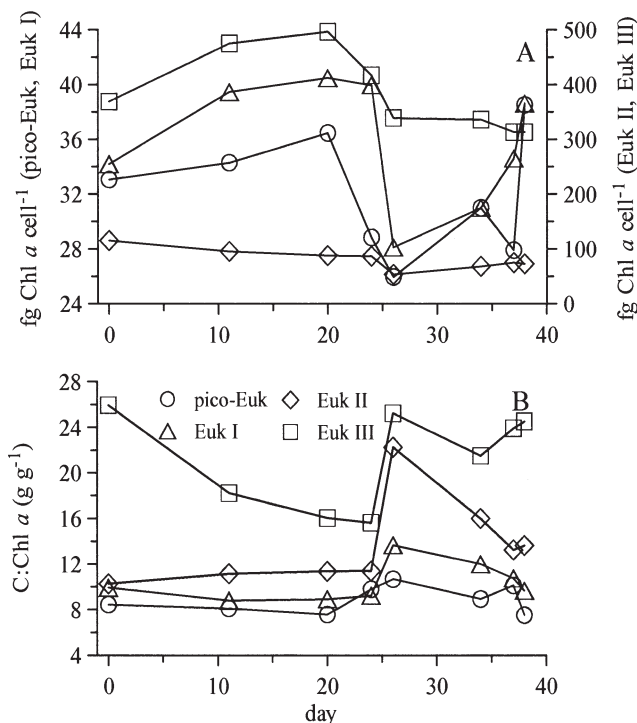


Fig. 5. (A) Estimated cellular Chl *a* concentration and (B) the ratio of C : Chl *a* of the four phytoplankton groups identified by flow cytometry inside the fertilized patch at 20-m depth.

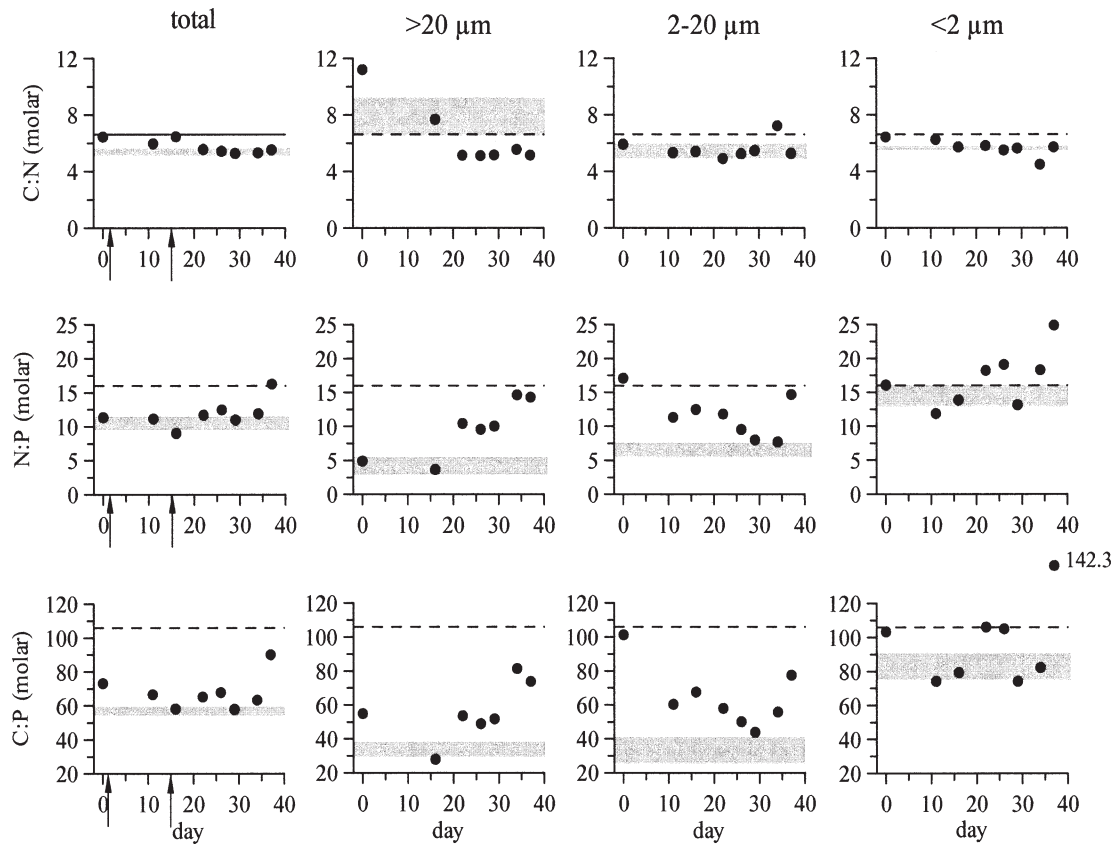


Fig. 6. Elemental composition of the total community and of the micro- ($>20\ \mu\text{m}$), nano- ($2\text{--}20\ \mu\text{m}$), and picoplankton ($<2\ \mu\text{m}$) at 20-m depth. The grey area represents the mean and standard deviation of three out-stations. The dashed line represents the Redfield ratio, and arrows indicate days of iron fertilization.

same trend as the N : P ratios, which indicates that the changes are mainly driven by variations in POP concentrations. The C : P ratio of the nanoplankton decreased from 101.3 to 43.9 at day 29 and increased again at the last station to 77.5 inside the fertilized patch. Outside the patch, the ratio was about 33. The microplankton C : P ratio was 54.9 at the initial station, decreased to 27.9 at day 16, and increased to 81.3 at day 34, while they were about 34 at the out-stations. Generally, the N : P and C : P ratios were extremely low in the $>20\ \mu\text{m}$ size fraction in unfertilized waters, rising after iron fertilization.

However, the elemental composition of the total community conceals these diverse responses of the individual size classes. Especially the two dominant size fractions, $>20\ \mu\text{m}$ and $2\text{--}20\ \mu\text{m}$, show an opposite trend for the N : P and C : P ratios, which almost cancelled each other out.

Shifts in composition of taxonomic groups—To distinguish between pico- ($<2\ \mu\text{m}$), nano- ($2\text{--}20\ \mu\text{m}$), and microphytoplankton ($>20\ \mu\text{m}$) reactions to iron fertilization, we analyzed changes in pigment composition of size-fractionated samples. The percentage of total Chl *a* within the different size classes (Fig. 7A,B) clearly shows different developments in smaller and larger organisms. Picophytoplankton contributed less than 20% of total Chl *a* before

fertilization and did not change much during the experiment (Fig. 7A). The dominant size class during the course of the experiment was nanophytoplankton, which accounted for 44% to 71% of total Chl *a*. Microphytoplankton showed the strongest biomass increase as seen in percent of total Chl *a* and carbon biomass (data not shown). It increased its relative amount from 12% to 46% of total Chl *a* between days 11 and 26 and decreased again thereafter.

The additional size fractionation performed for the HPLC pigment samples split the $2\text{--}20\text{-}\mu\text{m}$ fraction into $2\text{--}8$ and $8\text{--}20\ \mu\text{m}$ (Fig. 7B). Here, the $8\text{--}20\ \mu\text{m}$ was clearly the dominant fraction within the nanophytoplankton group, while the $2\text{--}8\text{-}\mu\text{m}$ fraction only accounted for less than 20% of total Chl *a* in the beginning and decreased to less than 10% during the experiment. The additional fragmentation of the $<2\text{-}\mu\text{m}$ fraction into $<0.8\ \mu\text{m}$ and $0.8\text{--}2\ \mu\text{m}$ did not show any changes. This relative contribution of Chl *a* by different size classes was also confirmed by the flow cytometer-derived chlorophyll measurements (for the fractions $<20\ \mu\text{m}$, data not shown).

HPLC pigment measurements showed that fucoxanthin and chlorophyll *c* 1.2 (Chl *c* 1.2) were the most abundant pigments after Chl *a* in the microphytoplankton (Fig. 8A). The absolute concentration of both increased more than 13 times through day 26 from 65.5 to 886.6 ng L^{-1} for

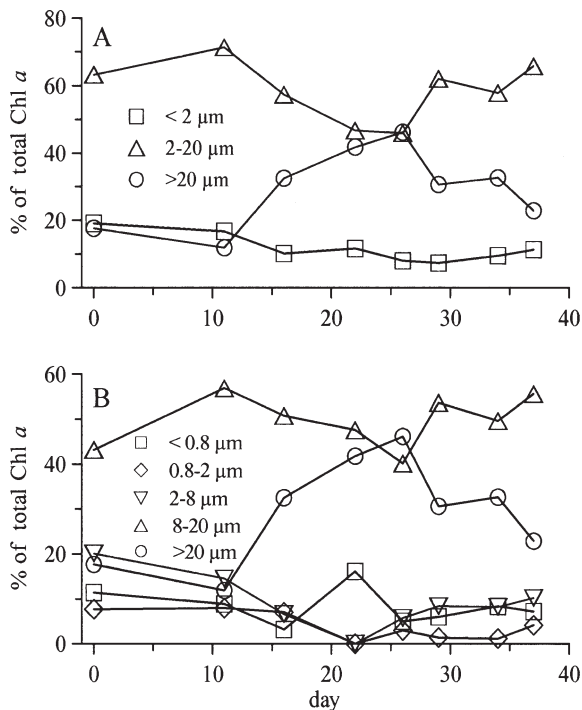


Fig. 7. Percentage of total Chl *a* at 20-m depth (A) inside the fertilized patch of the pico- ($< 2 \mu\text{m}$), nano- ($2-20 \mu\text{m}$), and microphytoplankton ($>20 \mu\text{m}$), and (B) inside the fertilized patch of two groups of the picophytoplankton ($< 0.8 \mu\text{m}$ and $0.8-2 \mu\text{m}$), two groups of the nanophytoplankton ($2-8 \mu\text{m}$ and $8-20 \mu\text{m}$), and the microphytoplankton ($>20 \mu\text{m}$).

fucoxanthin and from 18.6 to 272.7 ng L^{-1} for Chl *c* 1.2. Chl *c* 1.2 is the marker pigment of the group of chromophytes consisting of dinoflagellates, pelagophytes, cryptophytes, and diatoms. Fucoxanthin is a marker pigment, which mainly occurs in diatoms. The ratio of fucoxanthin to Chl *a* was very high throughout the experiment, ranging between 0.56 and 0.87, which indicates that the microphytoplankton size fraction consisted primarily of diatoms. Chlorophyll *c* 3 (Chl *c* 3) and 19-hexanoyloxyfucoxanthin (19-hex) increased in concentration from 4.8 to 90.2 ng L^{-1} for Chl *c* 3 and from 7.6 to 26.9 ng L^{-1} for 19-hex. Both pigments are markers for haptophytes. Haptophytes are small cells, belonging to the pico- or nanophytoplankton. Therefore, they must have been present in the colonial form of the haptophyte type *Phaeocystis* to be found in the $>20 \mu\text{m}$ size class at the beginning of the experiment.

The $2-8 \mu\text{m}$ size fraction was only a minor part of the total Chl *a* (5.7–20.1%; Fig. 7B), and absolute Chl *a* concentrations only doubled. But unlike all other size fractions, it is striking that the other pigments did not follow the same trend as Chl *a* (Fig. 8B). Fucoxanthin increased almost 8.7 times, while 19-hex, the most abundant pigment after Chl *a* in the beginning, almost halved. This resulted in fucoxanthin being the most abundant pigment next to Chl *a* after day 22 (see arrow in Fig. 8B). The marker pigment of pelagophytes 19-butanoyloxyfucoxanthin (19-but), decreased 1.8 times, while all other pigments showed almost no changes.

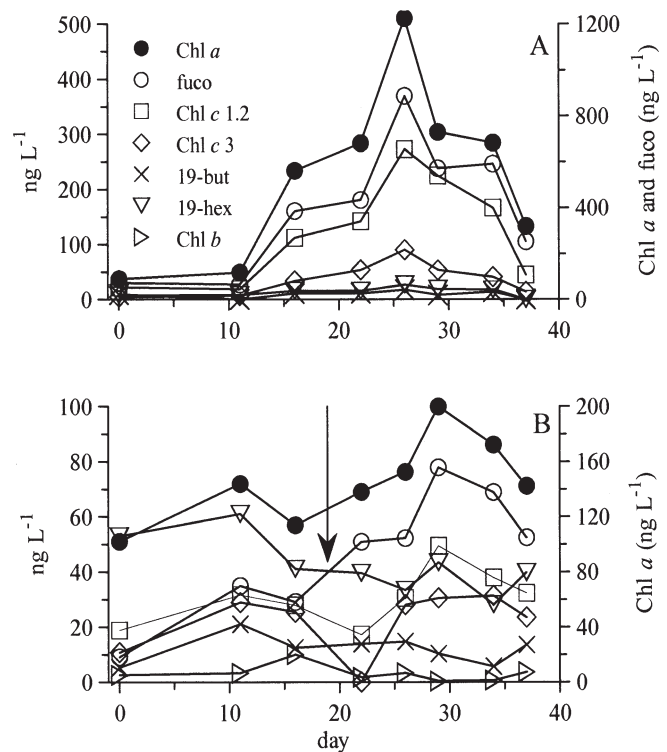


Fig. 8. Pigment composition at 20-m depth of (A) the $>20 \mu\text{m}$ size fraction and (B) the $2-8 \mu\text{m}$ size fraction. The arrow indicates the shift from high 19-hex to high fucoxanthin concentrations between days 16 and 22.

Relative changes in the proportion of five marker pigments are summarized in Fig. 9. They clearly show the massive fucoxanthin increase in the $8-20 \mu\text{m}$ and $>20 \mu\text{m}$ fractions. However, in both size fractions, fucoxanthin was the dominant pigment from the beginning, while in the $2-8 \mu\text{m}$ fraction, there was a shift from high 19-hex to high fucoxanthin concentrations. This relative increase of the marker pigment of diatoms was mainly caused by the overwhelming increase in the absolute fucoxanthin concentrations in every size fraction larger than $2 \mu\text{m}$.

Microscopic cell counts of the small diatom species *Fragilariopsis cylindrus*, *Cylindrotheca closterium*, *Chaetoceros* sp. (solitary cells), and an unidentified small pennate diatom as well as the two haptophytes, *Phaeocystis antarctica* (solitary cells) and *Emiliania huxleyi*, which all fit into the $2-8 \mu\text{m}$ size fraction, also showed a higher increase of the diatoms than the haptophytes after day 22 (Fig. 10).

Discussion

Biomass response to iron fertilization—During EIFEX, the fifth in situ iron fertilization experiment in the Southern Ocean, we induced a massive phytoplankton bloom in austral fall. The 5.3-fold increase in Chl *a* concentration (Fig. 1) was of the same magnitude as in the two Southern Ocean in situ iron-fertilization experiments SOIREE (6-fold) and EisenEx (about 4.6-fold) (Boyd et al. 2000; Gervais et al. 2002). The SOFEX North and South

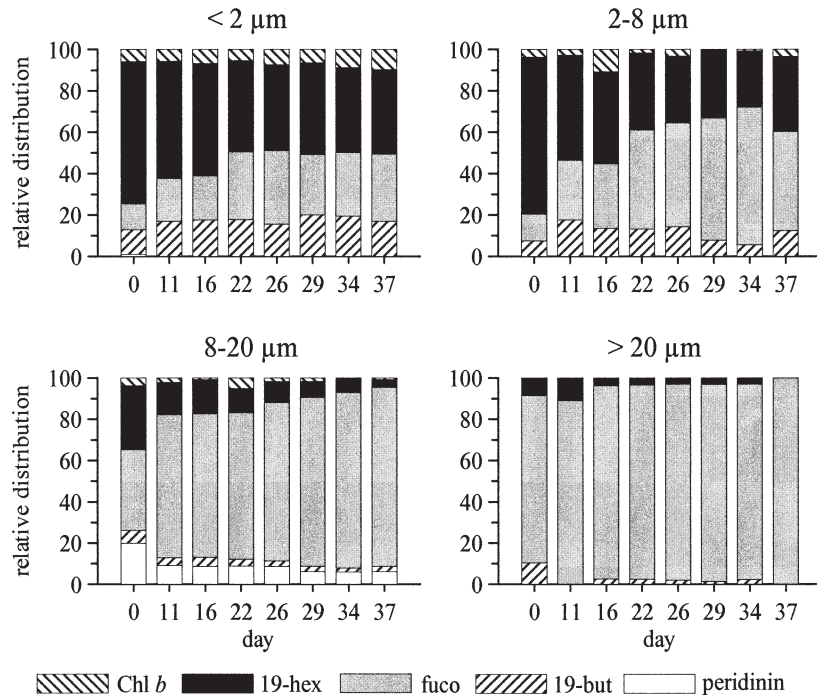


Fig. 9. Relative distributions of the marker pigments chlorophyll *b* (Chl *b*, chlorophytes), 19-hexanoyloxyfucoxanthin (19-hex, haptophytes), fucoxanthin (diatoms), 19-butanoyloxyfucoxanthin (19-but, pelagophytes), and peridinin (dinoflagellates) in the four size classes: $<2 \mu\text{m}$, $2\text{--}8 \mu\text{m}$, $8\text{--}20 \mu\text{m}$, and $>20 \mu\text{m}$ at 20-m depth.

experiments showed higher Chl *a* increases (10- and 20-fold), which were mostly due to the lower prefertilization concentrations (Coale et al. 2004). The maximum Chl *a* concentration in 20-m depth of more than $2,800 \text{ ng L}^{-1}$ reached during EIFEX were higher than those measured during SOIREE (about $1,800 \text{ ng L}^{-1}$), EisenEx ($2,310 \text{ ng L}^{-1}$), and SOFEX North (about $2,600 \text{ ng L}^{-1}$), but lower than those found at SOFEX South (about $3,800 \text{ ng L}^{-1}$; Boyd et al. 2000; Gervais et al. 2002; Coale et

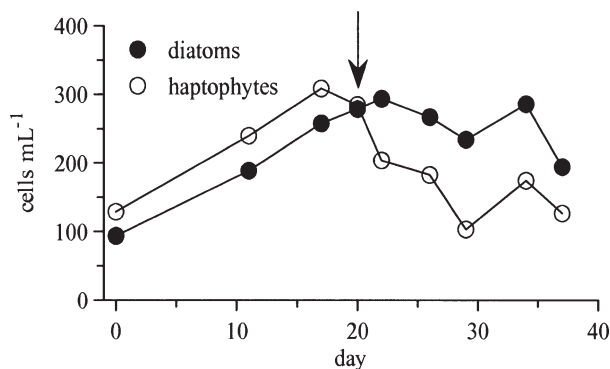


Fig. 10. Cell numbers of the diatom species *Fragilariopsis cylindrus*, *Cylindrotheca closterium*, *Chaetoceros* sp. (solitary cells), one unidentified small pennate diatom, and the two haptophytes species *Phaeocystis antarctica* (solitary cells) and *Emiliania huxleyi* in the $2\text{--}8\text{-}\mu\text{m}$ size fraction at 20-m depth. The arrow indicates the shift from higher haptophyte cell numbers to higher diatom cell numbers at day 20.

al. 2004). The decline in the Chl *a*, POC, PON, and POP concentrations toward the end of the experiment suggests the demise of the iron-induced bloom (Figs. 1 and 2). This is in contrast with previous shorter experiments, where the phytoplankton biomass remained high until the end of the observations.

The POC, PON, and POP data result from measurements of the total particulate material and include autotrophic as well as heterotrophic biomass. An interpretation of changes in the autotrophic community from these parameters alone is therefore not unequivocal. However, all particulate organic matter components showed similar temporal patterns as Chl *a*, indicating that these changes are dominated by phytoplankton development. A similar trend was found during EisenEx, where Chl *a*, POC, and PON concentrations at 20-m depth inside the fertilized patch increased constantly until day 21 (Riebesell pers. comm.).

The strong decline in the POC : Chl *a* ratio of the whole plankton community inside the iron-enriched patch indicated a proportional increase in autotrophic biomass relative to the heterotrophic plankton component (Fig. 3). A similar trend was observed during SOIREE and EisenEx, where the POC : Chl *a* ratio was reduced by a factor of two in a time span of 13 days (Boyd et al. 2000) and by a factor of 4.4 within 21 days (Riebesell pers. comm.). To some extent, this could have been due to enhanced chlorophyll synthesis upon iron repletion (chlorosis; Geider and LaRoche 1994). In cultures of the diatom *Phaeodactylum tricorutum*, cellular Chl *a* concentrations increased by

Table 3. Changes in the absolute (ng L^{-1}) and relative (% of total) amounts of Chl *a* of the pico- ($<2 \mu\text{m}$), nano- ($2\text{--}20 \mu\text{m}$), and microphytoplankton ($>20 \mu\text{m}$) during the first 26 (*29) days of EIFEX and 21 days of EisenEx (Gervais et al. 2002). EIFEX samples were taken from 20-m depth and EisenEx data are mean values of all measurements between 0 m and 80 m.

Size fraction	EIFEX (ng L^{-1})	EisenEx (ng L^{-1})	EIFEX (% of total)	EisenEx (% of total)
$>20 \mu\text{m}$	89.7 \rightarrow 1,225	50 \rightarrow 1,100	12 \rightarrow 46	10 \rightarrow 43
$2\text{--}20 \mu\text{m}$	321.5 \rightarrow 1,477*	250 \rightarrow 1,100	63.2 \rightarrow 45.9	50 \rightarrow 44
$<2 \mu\text{m}$	97.2 \rightarrow 212.7	200 \rightarrow 300	± 15	42 \rightarrow 13

a factor of 4.4 and the ratio POC : Chl *a* decreased by a factor of 3.2 upon iron addition (Greene et al. 1991). Also during the present survey, the cellular Chl *a* content determined by flow cytometry increased slightly in the picophytoplankton group pico-Euk and Euk I and the nanophytoplankton group Euk III through day 20 (Fig. 5). Using the same method during EisenEx, cellular Chl *a* values were found to increase by a factor of two for the picophytoplankton community and up to a factor of four for the nanophytoplankton (Veldhuis and Timmermans unpubl. data). The small increase in cellular Chl *a* content observed during EIFEX cannot explain the strong decrease in POC : Chl *a*. Therefore, the observed decline in the total plankton carbon to phytoplankton chlorophyll ratio was predominantly due to preferential increase of mainly larger phytoplankton relative to the heterotrophic community.

BPSi can be used as an indicator for diatom biomass, as cell numbers of other organisms bearing silicious skeletons, like radiolarians, were insignificant compared with diatoms during EIFEX (Henjes pers. comm.). Surprisingly, the bPSi concentration did not decline toward the end of our observation (Fig. 2), while the diatom abundance, as determined by pigment measurements and cell counts, decreased after day 26 (Fig. 4A). A relative increase in the abundance of full cells and broken and empty frustules of heavily silicified diatoms compared with total diatom cell numbers was observed toward the end of the experiment (Table 2). This may be the cause for the slight increase in total bPSi concentration while total diatom cell numbers decreased. This assumption is also supported by the bPSi : POC ratio of the total community that increased from 0.24 to 0.5 during the experiment (Table 2).

Iron-induced growth in different size classes—A shift in the phytoplankton size distribution toward larger cells as a result of iron fertilization has been described for different HNLC regions (Cavender-Bares et al. 1999; Gervais et al. 2002; Eldridge et al. 2004). Cavender-Bares et al. (1999) found a dramatic change from a picoplankton-dominated community to one dominated by diatoms larger than $10 \mu\text{m}$ within 1 week in the equatorial Pacific. These findings are comparable with those of in situ iron-fertilization experiments in the Southern Ocean, despite the large physicochemical and biological differences of the two areas. During SOIREE, the first iron-fertilization experiment performed in the Southern Ocean in austral fall, the phytoplankton community was dominated by picoplankton (40% of total Chl *a* integrated over 65-m depth) before iron fertilization, while micro- and nanoplankton

both contributed 30% (Gall et al. 2001a). During the 13 days of the experiment, microphytoplankton Chl *a* concentrations increased by one order of magnitude, nanoplankton sixfold, and picoplankton threefold. Gall et al. (2001b) showed that nano- and microphytoplankton increased their primary production strongly while picophytoplankton primary production did not change much.

The absolute and relative changes in the nano- and microphytoplankton during EIFEX, conducted during austral fall, and a previous iron fertilization experiment in the Southern Ocean (EisenEx), conducted during austral spring, show generally similar developments (Table 3). There are some differences in the changes of picoplankton, which had twice as high Chl *a* concentration at the start of EisenEx compared with EIFEX. The initial Chl *a* concentrations of the nano- and microphytoplankton were both higher during EIFEX. Another difference is that, while the Chl *a* increase of the nanophytoplankton was similar in both experiments (factor of 4.6 during EIFEX and 4.4 during EisenEx), the microphytoplankton increased its biomass much more during EisenEx (22 times) compared with EIFEX (13.7 times). The difference in the rate of microphytoplankton biomass increase between the two experiments was mainly due to a stronger response of the fast-growing diatom species *Pseudo-nitzschia lineola* during EisenEx than EIFEX, based on microscopic cell counts (Assmy unpubl. data). Irrespective of the absolute and relative initial composition of the phytoplankton community, iron fertilization induced a massive increase of microphytoplankton biomass independent of the season. The amount of pico- and nanophytoplankton growth seems to be less stimulated by iron addition and may also be strongly dependent on grazing pressure. The latter may exert a strong influence but cannot be evaluated from our data.

Stimulation of diatoms by iron fertilization—The pigment fucoxanthin is mainly found in diatoms and therefore is used as a marker pigment for diatom biomass. However, fucoxanthin can be found in other phytoplankton groups as well, such as haptophytes (van Leeuwe and Stefels 1998). They describe that the fucoxanthin content of *Phaeocystis* increases due to iron fertilization. Part of the increasing fucoxanthin concentration found in the $2\text{--}8\text{-}\mu\text{m}$ fraction (size of solitary *Phaeocystis* cells) and in the $>20\text{-}\mu\text{m}$ fraction (size of *Phaeocystis* colonies) may therefore result from *Phaeocystis* instead of diatom growth. As microscopic cell counts showed that diatoms clearly dominated the microphytoplankton during EIFEX (Assmy et al. 2005), we

assume that this is of minor importance for the $>20\text{-}\mu\text{m}$ size fraction. In the $2\text{--}8\text{-}\mu\text{m}$ size fraction, the Chl *c* 1.2 concentration increased as well as the fucoxanthin concentration (Fig. 8B). Chl *c* 1.2 is only found in the group of chromophytes (diatoms, dinoflagellates, pelagophytes, and cryptophytes), but not in haptophytes. We conclude that the increase in fucoxanthin was therefore primarily caused by rising diatom concentrations. The fucoxanthin concentration overtook the 19-hex concentration (indicator for haptophytes) after day 22. This suggests that, before iron fertilization, mainly haptophytes were present, which were exceeded by diatoms from day 22 on. Apart from pigment analysis, cell counts support these findings and show that diatoms between $2\text{-}\mu\text{m}$ and $8\text{-}\mu\text{m}$ size increased their abundance stronger than haptophytes of the same size (Fig. 10). Gall et al. (2001a) describe similar and more pronounced changes in the composition of the whole phytoplankton community during SOIREE. Initially, the haptophyte type *Phaeocystis*, as determined by HPLC pigment measurements, dominated the total phytoplankton community. After an initial increase of these algae, diatoms became the dominant group about 1 week after iron fertilization.

Size-fractionated pigment analysis and microscopic cell counts (Assmy et al. 2005) indicated that diatoms $>20\text{ }\mu\text{m}$ were the main beneficiaries of iron addition during EIFEX, leading to a massive growth of long, chain-forming diatoms. This corresponds very well with other field data and incubation experiments after iron enrichment (Hutchins and Bruland 1998; Boyd et al. 2000; Gervais et al. 2002). The reason for this is thought to be the higher iron requirement of large cells due to the lower surface-to-volume ratio compared with smaller ones (Sunda and Huntsman 1995; Timmermans et al. 2001, 2004). Nevertheless, our pigment data suggest that iron fertilization stimulates diatom growth not only in the $>20\text{-}\mu\text{m}$ size class, but in every size fraction larger than $2\text{ }\mu\text{m}$ (Fig. 9). The ratio of fucoxanthin to Chl *a* increased 4.4 times in the $2\text{--}8\text{-}\mu\text{m}$ size fraction, while the increase was smaller in the $8\text{--}20\text{-}\mu\text{m}$ size fraction (1.6). This implies that even the very small diatoms enhance their growth rates due to iron fertilization. In the microphytoplankton, a massive growth of long, chain-forming diatoms occurred, but it did not change the relative group composition because diatoms were already dominant at the start of the experiment.

During EIFEX, diatoms dominated the phytoplankton community already prior to the fertilization experiment under iron-limiting conditions, and they were able to increase their biomass to a greater extent than other phytoplankton groups when iron became available (Fig. 4). The reason why diatoms in general tend to have an advantage over other phytoplankton groups under high nutrient conditions is thought to be their relatively high half-saturation constants (Sarhou et al. 2005). This is often explained by a low surface-to-volume ratio, which is only true for large cells but not for diatoms in general. Laboratory experiments with a large (*Chaetoceros dichchaeta*) and a small (*C. brevis*) Southern Ocean diatom species showed that *C. brevis* could not increase its growth rate with increasing iron availability (Timmermans et al. 2001),

which is in contrast with our findings. Hence, the success of diatoms under iron-rich conditions may not only be because of high half-saturation constants but may be caused by several adaptive strategies. First, diatoms have a generally better ability to take up and store iron compared with other taxonomical groups. Sunda and Huntsman (1995) describe that diatoms were able to accumulate iron and reach Fe : C values that were 20–30 times higher than those needed for maximal growth, while coccolithophores and dinoflagellates had only two to three times higher Fe : C values than required for optimal growth. Such luxury uptake of iron can be a major advantage in regions where iron is only temporarily available. This could allow diatoms to keep higher growth rates while total iron concentrations in the surrounding water are depleted. Second, diatoms are better protected against grazing pressure by their silica frustules compared with other, naked phytoplankton groups.

Changes in the elemental composition—The increasing N : P and C : P ratios of the microphytoplankton as a result of increased iron availability is a phenomenon that has been previously described in the literature (de Baar et al. 1997). The opposite trend within the nanophytoplankton through day 29 and the increase thereafter has, to our knowledge, not been described yet and is likely due to a shift in the group composition in this size class. This is indicated by strong changes in the marker pigment distribution of the whole nanophytoplankton and especially the $2\text{--}8\text{-}\mu\text{m}$ size fraction as well as by cell counts of the latter size fraction as described above.

Klausmeier et al. (2004) show that the N : P ratios of different freshwater and marine species range between 7.1 and 43.3, although the median of 17.7 was close to Redfield. The elemental composition of phytoplankton can vary over a wide range between species or functional groups, and diatoms in general have lower than Redfield N : P and C : P ratios, ranging between 9.3–14.1 and 62–100, respectively (Arrigo et al. 1999; Quigg et al. 2003; Ho et al. 2004). Arrigo et al. (1999, 2002) describe that waters of the Southern Ocean that are dominated by diatoms have lower than Redfield N : P and C : P ratios of the above-said range, while those dominated by the haptophyte *Phaeocystis antarctica* exceed the Redfield ratio and range between 17.2 and 19.5 for N : P and 120 and 154 for C : P. This is assumed to be caused by luxury P uptake and the formation of internal P pools in diatoms as a response to iron stress (Tremblay and Price unpubl.). The observed decrease in the N : P and C : P ratios of the nanoplankton may therefore be primarily due to a species shift from haptophytes to diatoms. Furthermore, it could explain why the N : P and C : P ratios of the microphytoplankton, which mainly consisted of diatoms, were already far below those of the nano- and picoplankton at the start of the experiment.

The increasing N : P and C : P ratios of the microphytoplankton cannot be explained by a shift in assemblage composition, as pigment data and cell counts indicate that this size fraction was dominated by diatoms from the beginning. However, species-specific shifts within the

diatom assemblage, as observed during EIFEX, might impact these ratios. It is likely that there are different adaptation strategies of smaller and larger phytoplankton species to iron limitation that result in different elemental compositions. Additionally, nitrate uptake is inhibited under iron limitation (Franck et al. 2003) because the enzymes essential for nitrate uptake, nitrate and nitrite reductase, are iron rich (Timmermans et al. 1994). Low nitrate uptake and the possible formation of internal P pools (Tremblay and Price unpubl.) result in a low N : P ratio under low iron concentrations. With iron fertilization, the growth rates of large diatoms increase in culture experiments (Timmermans et al. 2004) and in situ fertilization experiments. Increase in N uptake with iron fertilization (de Baar et al. 1997; Franck et al. 2003; Timmermans et al. 2004) and consumption of internal P reserves at enhanced growth rates may be the reason for the strong increase in N : P and C : P ratios in the microphytoplankton (Fig. 6).

Biogeochemical models assessing the carbon export from the upper ocean generally assume fixed elemental Redfield ratios in the exported organic material. Our investigations showed that the mean C : N and C : P ratios of the total community inside the fertilized patch were 13% and 36% lower than the Redfield ratio. This would result in a significant overestimation of the carbon export based on N or P uptake. Our data indicate that iron fertilization causes more changes, especially in the species composition of the small phytoplankton community, than hitherto assumed. Part of this change is likely to be caused by grazing. As the microphytoplankton is generally too large to be consumed by most microzooplankton grazers and too fast growing for mesozooplankton grazers when iron becomes available (Coale et al. 1996), mainly smaller phytoplankton groups are exposed to grazing pressure. Changes in the pico- and nanophytoplankton community structure and elemental ratios and, thus, changes in the main food source of microzooplankton grazers will have impacts on the composition of fecal pellets. Besides cell aggregates, fecal pellets are an important transport mechanism of carbon to the deep ocean after a phytoplankton bloom. Recent biogeochemical models consider different phytoplankton groups and size classes (Pasquer et al. 2005) and, hence, a detailed understanding of mechanisms influencing the elemental composition of all phytoplankton size classes is important.

The question remains whether the short-term changes observed by these investigations also apply for long-term iron fertilization. If continuous iron input would generally alter the composition of the phytoplankton community and size classes, the export of nutrients from the upper water column would be different from the present iron-limited situation. The observed slight increase in N : P and C : P ratios would indicate a lesser export of P and perhaps a higher export of N. However, these assumptions do not take into account potential changes in grazing pressure from micro- to mesozooplankton that may result from prolonged iron fertilization, and therefore the combined effects on the nutrient export are difficult to predict.

References

- ARRIGO, K. R., R. B. DUNBAR, M. P. LIZOTTE, AND D. H. ROBINSON. 2002. Taxon-specific differences in C/P and N/P drawdown for phytoplankton in the Ross Sea, Antarctica. *Geophys. Res. Lett.* **29** [doi:10.1029/2002GL015277].
- , D. H. ROBINSON, D. L. WORTHEM, R. B. DUNBAR, G. R. DiTULLIO, M. VANWORT, AND M. P. LIZOTTE. 1999. Phytoplankton community structure and the drawdown of nutrients and CO₂ in the Southern Ocean. *Science* **283**: 365–367.
- ASSMY, P., J. HENJES, K. SCHMIDT, V. SMETACEK, AND M. MONTRESOR. 2005. The wax and wane of an iron-induced diatom bloom in the Southern Ocean. *Berichte zur Polar und Meeresforschung* **500**: 89–100.
- BARLOW, R. G., D. G. CUMMINGS, AND S. W. GIBB. 1997. Improved resolution of mono- and divinyl chlorophylls *a* and *b* and zeaxanthin and lutein in phytoplankton extracts using phase C-8 HPLC. *Mar. Ecol. Prog. Ser.* **161**: 303–307.
- BOYD, P. W., AND OTHERS. 2000. A mesoscale phytoplankton bloom in the polar Southern Ocean stimulated by iron fertilization. *Nature* **407**: 695–702.
- CAVENDER-BARES, K. K., E. L. MANN, S. W. CHISHOLM, M. E. ONDRUSEK, AND R. R. BIDIGARE. 1999. Differential response of equatorial Pacific phytoplankton to iron fertilisation. *Limnol. Oceanogr.* **44**: 237–246.
- CEMBELLA, C., H. ROHR, K. LOQUAY, AND V. STRASS. 2005. Mapping horizontal spreading of a developing phytoplankton bloom using an airborne chlorophyll *a* fluorescence LIDAR. *Berichte zur Polar und Meeresforschung* **500**: 38–43.
- COALE, K. H., AND OTHERS. 1996. A massive phytoplankton bloom induced by an ecosystem-scale iron fertilization experiment in the equatorial Pacific Ocean. *Nature* **383**: 495–501.
- , AND OTHERS. 2004. Southern Ocean iron enrichment experiment: Carbon cycling in high- and low-Si waters. *Science* **304**: 408–414.
- DE BAAR, H. J. W., M. A. VAN LEEUWE, R. SCHAREK, L. GOEYENS, K. M. J. BAKKER, AND P. FRITSCH. 1997. Nutrient anomalies in *Fragilariopsis kerguelensis* blooms, iron deficiency and the nitrate/phosphate ratio (A. C. Redfield) of the Antarctic Ocean. *Deep-Sea Res. II* **44**: 229–260.
- , AND OTHERS. 2005. Synthesis of iron fertilisation experiments: From the Iron Age in the age of enlightenment. *J. Geophys. Res.* **110**. C09S16, [doi:10.1029/2004JC002601].
- EHRHARD, M., AND W. KOEVE. 1999. Determination of particulate organic carbon and nitrogen, p. 437–444. *In* K. Grasshoff, K. Kremling and M. Ehrhard [eds.], *Methods of seawater analysis*. Wiley-VCH.
- ELDRIDGE, M. L., AND OTHERS. 2004. Phytoplankton community response to a manipulation of bioavailable iron in HNLC waters of the subtropical Pacific Ocean. *Aquat. Microb. Ecol.* **35**: 79–91.
- FRANCK, V. M., K. W. BRULAND, D. A. HUTCHINS, AND M. A. BRZEZINSKI. 2003. Iron and zinc effects on silicic acid and nitrate uptake kinetics in three high-nutrient, low-chlorophyll (HNLC) regions. *Mar. Ecol. Prog. Ser.* **252**: 15–33.
- GALL, M. P., P. W. BOYD, J. HALL, K. A. SAFI, AND H. CHANG. 2001a. Phytoplankton processes. Part 1: Community structure during the Southern Ocean Iron Release Experiment (SOIREE). *Deep-Sea Res. Part II* **48**: 2551–2570.
- , R. STRZEPEK, M. MALDONADO, AND P. W. BOYD. 2001b. Phytoplankton processes. Part 2. Rates of primary production and factors controlling algal growth during the Southern Ocean Iron Release Experiment (SOIREE). *Deep-Sea Res. Part II* **48**: 2571–2590.

- GEIDER, R. J., AND J. LAROCHE. 1994. The role of iron in phytoplankton photosynthesis, and the potential for iron-fertilization of primary productivity in the sea. *Photosynthesis Res.* **39**: 275–301.
- , AND ———. 2002. Redfield revisited: Variability of C : N : P in marine microalgae and its biogeochemical basis. *Eur. J. Phycol.* **37**: 1–17.
- GERVAIS, F., U. RIEBESELL, AND M. Y. GORBUNOV. 2002. Changes in primary productivity and chlorophyll *a* in response to iron fertilization in the Southern Polar Frontal Zone. *Limnol. Oceanogr.* **47**: 1324–1335.
- GREENE, R. M., R. J. GEIDER, AND P. G. FALKOWSKI. 1991. Effect of iron on photosynthesis in a marine diatom. *Limnol. Oceanogr.* **36**: 1772–1782.
- HANSEN, H. P., AND F. KOROLEFF. 1999. Determination of nutrients, p. 159–228. *In* K. Grasshoff, K. Kremling and M. Ehrhard [eds.], *Methods of seawater analysis*. Wiley-VCH.
- HO, T. Y., A. QUIGG, Z. V. FINKEL, A. J. MILLIGAN, K. WYMAN, P. G. FALKOWSKI, AND F. M. M. MOREL. 2004. The elemental composition of some marine phytoplankton. *J. Phycol.* **39**: 1145–1159.
- HUDSON, R. J. M., AND F. M. M. MOREL. 1990. Iron transport in marine phytoplankton: Kinetics of cellular and medium coordination reactions. *Limnol. Oceanogr.* **35**: 1002–1020.
- HUTCHINS, D. A., AND K. W. BRULAND. 1998. Iron-limited diatom growth and Si : N uptake ratios in a coastal upwelling regime. *Nature* **393**: 561–564.
- KLAUSMEIER, C. A., E. LITCHMAN, T. DAUFRESNE, AND S. A. LEVIN. 2004. Optimal nitrogen-to-phosphorus stoichiometry of phytoplankton. *Nature* **429**: 171–174.
- MACKEY, M. D., D. J. MACKEY, H. W. HIGGINS, AND S. W. WRIGHT. 1996. CHEMTAX—a program for estimating class abundances from chemical markers: Application to HPLC measurements of phytoplankton. *Mar. Ecol. Prog. Ser.* **14**: 265–283.
- MARTIN, J. H., S. E. FITZWATER, AND R. M. GORDON. 1990. Iron deficiency limits phytoplankton growth in Antarctic waters. *Global Biogeochem. Cycles* **4**: 5–12.
- PASQUER, B., G. LARUELLE, S. BECQUEVORT, W. SCHOEMANN, H. GOOSSE, AND C. LANCELOT. 2005. Linking ocean biogeochemical cycles and ecosystem structure and function: Results of the complex SWAMCO-4 model. *J. Sea Res.* **53**: 93–108.
- QUIGG, A., AND OTHERS. 2003. The evolutionary inheritance of elemental stoichiometry in marine phytoplankton. *Nature* **425**: 291–294.
- RÖTTGERS, R., F. COLIJN, AND M. DIBBERN. 2005. Algal physiology and biooptics. *Berichte zur Polar und Meeresforschung* **500**: 82–88.
- SARTHOU, G., K. R. TIMMERMANS, S. BLAIN, AND P. TREGUER. 2005. Growth physiology and fate of diatoms in the ocean: A review. *J. Sea Res.* **53**: 25–42.
- SUNDA, W. G., AND S. A. HUNTSMAN. 1995. Iron uptake and growth limitation in oceanic and coastal phytoplankton. *Mar. Chem.* **50**: 189–206.
- , AND ———. 1997. Interrelated influence of iron, light and cell size on marine phytoplankton growth. *Nature* **390**: 389–392.
- TIMMERMANS, K. R., W. STOLTE, AND H. J. W. DE BAAR. 1994. Iron-mediated effects on nitrate reductase in marine phytoplankton. *Mar. Biol.* **121**: 389–396.
- , B. VAN DER WAGT, AND H. J. W. DE BAAR. 2004. Growth rates, half saturation constants, and silicate, nitrate, and phosphate depletion in relation to iron availability of four large open-ocean diatoms from the Southern Ocean. *Limnol. Oceanogr.* **49**: 2141–2151.
- , AND OTHERS. 2001. Growth rates of large and small Southern Ocean diatoms in relation to availability of iron in natural seawater. *Limnol. Oceanogr.* **46**: 260–266.
- TWINING, B. S., S. B. BAINES, AND N. S. FISHER. 2004. Element stoichiometries of individual plankton cells collected during the Southern Ocean Iron Experiment (SOFEX). *Limnol. Oceanogr.* **49**: 2115–2128.
- UTERMÖHL, H. 1958. Zur Vervollkommnung der quantitativen Phytoplankton-Methodik. *Mitt. int. Verein. theor. angew. Limnol.* **9**: 1–38.
- VAN LEEUWE, M. A., AND J. STEFELS. 1998. Effects of iron and light stress on the biogeochemical composition of Antarctic *Phaeocystis* sp. (Prymnesiophyceae). II. Pigment composition. *J. Phycol.* **34**: 496–503.
- VAULOT, D., C. COURTIES, AND F. PARTENSKY. 1989. A simple method to preserve oceanic phytoplankton for flow cytometric analyses. *Cytometry* **10**: 629–635.
- VELDHUIS, M. J. W., AND G. W. KRAAY. 2000. Application of flow cytometry in marine phytoplankton research: Current applications and future perspectives. *Sci. Mar.* **64**: 121–134.
- WALTER, S., I. PEEKEN, K. LOCHTE, A. WEBB, AND H. W. BANGE. 2005. Nitrous oxide measurements during EIFEX, the European Iron Fertilization Experiment in the subpolar South Atlantic Ocean. *Geophys. Res. Lett.* **32** [doi:10.1029/2005GL024619].
- WRIGHT, S. W., D. P. THOMAS, H. J. MARCHANT, H. W. HIGGINS, M. D. MACKEY, AND D. J. MACKEY. 1996. Analysis of phytoplankton of the Australian sector of the Southern Ocean: Comparisons of microscopy and size frequency data with interpretations of pigment HPLC data using the 'CHEMTAX' matrix factorisation program. *Mar. Ecol. Prog. Ser.* **144**: 285–298.
- ZIELINSKI, U., AND R. GERSONDE. 1997. Diatom distribution in Southern Ocean surface sediments (Atlantic sector): Implications for paleoenvironmental reconstructions. *Palaeogeogr. Palaeoclimatol. Palaeoecol.* **129**: 213–250.

Received: 12 July 2005

Amended: 19 December 2005

Accepted: 30 December 2005